J. MATER. CHEM., 1991, 1(2), 265–269

Electron Paramagnetic Resonance Spectroscopy of Cu^{+}/Cu^{2+} β''-Alumina

Didier Gourier,*[a] Daniel Vivien,[a] Bruce Dunn[b] and Lynn Salmon[b]
[a] *Laboratoire de Chimie Appliquée de l'Etat Solide, URA 302 ENSCP, 11 rue Pierre et Marie Curie, 75231 Paris cedex 05, France*
[b] *Department of Materials Sciences and Engineering, University of California, Los Angeles, CA 90024, USA*

Cu^{+}/Cu^{2+} β''-alumina single crystals have been studied by electron paramagnetic resonance (EPR) spectroscopy. The results indicate that Cu^{2+} ions are essentially found in an off-centre position in the conduction planes. The co-ordination polyhedron is a distorted square pyramid of C_2 symmetry. The magnetic parameters are found to be: $g_z=2.385$, $g_x=2.097$, $g_y=2.072$, $A_z=91\times10^{-4}$ cm^{-1}, $A_x\leq20\times10^{-4}$ cm^{-1} and $A_y=32\times10^{-4}$ cm^{-1}. Low concentrations of Cu^{2+} ions are also found in two other non-identified sites. Heat treatments in air at temperatures above 500 °C indicate that Cu^{2+} is reduced to Cu^{+}.

Keywords: *Cu^{+} β''-Alumina; Luminescent material; Electron paramagnetic resonance spectroscopy*

1. Introduction

Sodium β''-alumina is a well known superionic conductor whose highly anisotropic structure consists of close-packed 'spinel blocks' of Al, Mg and O separated by more open regions (the two-dimensional conduction planes) in which Na^{+} ion mobility is observed. The material is characterized by a rich ion-exchange chemistry, which gives rise to a variety of monovalent, divalent and trivalent isomorphs. The synthesis, structure and properties of the ion-exchanged β''-aluminas have been reviewed recently.[1,2]

The incorporation of lanthanide and transition-metal ions in β''-alumina has led to considerable interest in the optical properties that this solid electrolyte is capable of possessing. A variety of attractive properties have been observed including tunable emission, energy transfer, up-conversion, waveguiding and laser action. In general, the anisotropic structure of the β''-alumina with its loosely packed conduction plane represents a novel host environment for luminescent ions. This feature, in combination with the use of ion exchange to control independently the doping process, has enabled the β''-aluminas to exhibit unexpected optical effects and to be considered for several optical device applications.

Spectroscopy techniques have proven to be extremely useful for probing the structural arrangements present in lanthanide- and transition-metal-doped β''-aluminas. Optical absorption[3] and site-selective spectroscopy studies[4] have provided specific details concerning the local environment for Nd^{3+} and Eu^{3+} β''-aluminas, respectively. The information derived from these studies effectively complements that obtained from single-crystal X-ray diffraction.[5] Detailed knowledge concerning local environment is also available from EPR studies, which augment optical spectroscopy by providing information regarding the electronic ground state of the paramagnetic species. The combination of the two techniques provides particular insight when the paramagnetic species are also optically responsive, as demonstrated in the cases of Nd^{3+}- and Ce^{3+}-doped materials.[6,7]

The present work considers the properties of copper-doped β''-alumina. In the monovalent state, tunable luminescence was achieved over a wide range in the visible and optical gain was reported.[8] The fact that Cu^{+} is both mobile and luminescent has led to dynamic optical behaviour involving the formation of dimers and producing an optical memory effect.[9,10] The presence of Cu^{2+} in these materials is quite detrimental because the Cu^{2+} efficiently quenches Cu^{+} luminescence. The Cu^{2+} ion is paramagnetic ($3d^9$ configuration) and thus there is an opportunity to use EPR to identify the concentration of these ions and the thermal treatments that reduce the ion to the Cu^{+} state. In a previous EPR study of Na^{+}/Cu^{2+} β''-alumina, the Cu^{2+} were found to occupy mainly the mid-oxygen (mO) site in the conduction plane.[11] Annealing treatments were investigated and found to affect the EPR spectrum. In addition, changes in the spectra at temperatures above 4 K were attributed to ionic motion in the conduction plane.

The present study considers a different composition, Cu^{+}/Cu^{2+} β''-alumina. In this case the entire sodium content has been replaced by copper, producing a material whose monovalent component (*i.e.* Cu^{+}) has substantially lower mobility than that of Na^{+}. The EPR results identify the off-centre site occupied by Cu^{2+} and how the Cu^{2+} concentration decreases from specific thermal treatments.

2. Experimental

Single crystals of Na^{+}/Cu^{2+} β''-alumina with nominal composition $Na_{1.67}Mg_{0.67}Al_{10.33}O_{17}$ were prepared by the flux evaporation technique. They typically measured $5\times5\times0.2$ mm in size. Crystals of Cu^{+}/Cu^{2+} β''-alumina were obtained by ion-exchange techniques.[8,9] The precursor Na^{+} β''-alumina crystals were immersed in $CuCl_2$ melts at 640 °C under N_2 atmosphere for 3–9 h. $CuCl_2$ is not stable in the melt and decomposes according to the reaction $CuCl_2\rightarrow CuCl+\frac{1}{2}Cl_2$. As a consequence, Na^{+} ions were exchanged by both Cu^{2+} and Cu^{+} ions. The replacement of copper for sodium was complete; residual Na^{+} ions could not be detected in the crystals by EDAX. After exchange, the crystals were uniformly brown in colour and slightly translucent. The brown colour was also observed in (polycrystalline) Cu^{+} β-alumina prepared by electrolysis.[12] The $Cu^{2+}:Cu^{+}$ ratio was not determined precisely, but the lack of exchange narrowing and the intensity of the EPR spectra indicated that the $Cu^{2+}:Cu^{+}$ ratio was *ca.* 5–10%.

The EPR spectra were recorded on a Bruker ER 220 D spectrometer equipped with a variable-temperature accessory (100–300 K). Low temperatures (4–100 K) were obtained with a helium-flow cryostat from Oxford Instruments.

3. Results and Discussion

The EPR spectrum of Cu^{2+} ($3d^9$ configuration) is composed of two sets of four hyperfine lines resulting from the existence of two magnetic isotopes (^{63}Cu, $I=3/2$, $g_N=1.484$, 69.2% and ^{65}Cu, $I=3/2$ $g_N=1.588$, 30.8%). In β''-alumina, however, EPR lines are generally very broad because of the strain broadening induced by structural disorder. As a result, it was not possible to identify contributions of the two copper isotopes in Cu^+/Cu^{2+} β''-alumina. Moreover, the hyperfine lines frequently overlap, especially for $B_0 \| c$, leading to a broad, unresolved EPR line (*vide infra*). In the present investigation, the Cu^{2+} EPR spectra were readily detectable over a very wide temperature range, extending from 4 K to room temperature. This behaviour is strikingly different from the EPR spectra of Na^+/Cu^{2+} β''-alumina which were well resolved only below 77 K.[11] Although the spectral resolution increases with decreasing temperature, for convenience the EPR was performed at the moderately low temperature of $T \approx 140$ K.

3.1 EPR for $B_0 \| c$ and Effects of Thermal Treatments

The EPR spectrum is very complicated for an arbitrary orientation of the magnetic field B_0 with respect to the crystallographic axes. The spectrum, however, is simplified considerably for $B_0 \| c$, and the general features of Cu^{2+} EPR in Cu^+/Cu^{2+} β''-alumina can be understood best by using this field orientation. For $B_0 \| c$, the EPR spectrum consists of a broad, structureless and asymmetric EPR line corresponding to Cu^{2+} ions in a site labelled Cu^{2+}(I) (Fig. 1). Small satellite peaks that are present in the high-field wing of the spectrum belong to Cu^{2+} located in another site labelled Cu^{2+}(II). By using appropriate estimations of spectral areas, it is evident that more than 90% of the divalent copper is located in the Cu^{2+}(I) site.

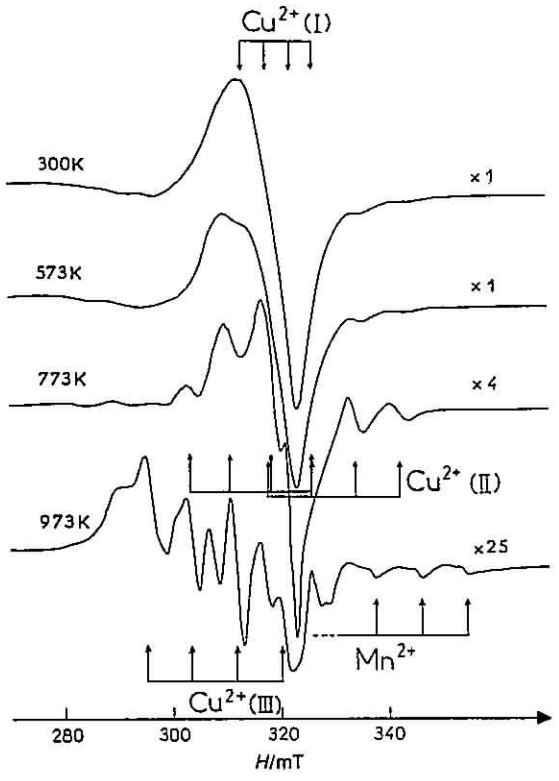

Fig. 1 EPR spectra at 140 K of Cu^+/Cu^{2+} β''-alumina. The magnetic field, B_0, is parallel to the crystallographic c axis. The spectra have been recorded in the unannealed sample and after annealing treatments in air for 20 h at 573, 773 and 973 K

The influence of annealing temperature on EPR response is also shown in Fig. 1. The spectral changes are consistent with the reduction of Cu^{2+} and analogous to the reduction observed for several other β''-aluminas including the Ag^+, Pb^{2+} and Sn^{2+} isomorphs.[13] The annealing treatments were performed in air for 20 h at several temperatures (573, 773, 973 and 1073 K). At 573 K, a small decrease in Cu^{2+}(I) intensity is observed, caused by a partial reduction of Cu^{2+}. This reduction is more severe at 773 K as *ca.* 75% of Cu^{2+}(I) is reduced. Note that Cu^{2+}(II) remains unaffected by these two thermal treatments. The two broad lines belonging to this site in the field range 330–340 mT are unchanged. Heat treatment at 973 K results in complete reduction of Cu^{2+}(I). Moreover, careful examination of the spectrum in the 330–360 mT range shows that the Cu^{2+}(II) is also almost completely reduced. The two broad lines mentioned above are no longer evident: the three narrow lines separated by 8 mT that are observed, arise from Mn^{2+} impurities. All the other lines in the 280–330 mT range are due to Cu^{2+} in another site labelled Cu^{2+}(III), which contributes by only a few percent to the total Cu^{2+} concentration. The treatment at 1073 K (not shown in Fig. 1) leads to complete reduction of Cu^{2+} and only the characteristic pattern of six hyperfine lines of the $|1/2> \rightarrow |-1/2>$ transition of Mn^{2+} impurities is detected.

Previous work has shown that several β''-alumina single-crystal isomorphs undergo reduction reactions when heated in inert gas or vacuum at temperatures in the vicinity of 900 K. Rohrer and Farrington determined that the presence of water in the β''-alumina conduction plane played an important role in this reaction.[13] Based on various hydration/dehydration experiments, they proposed that during heat treatment the water incorporated in the β''-alumina structure would diffuse from the bulk crystal and reduce the mobile species (*e.g.*, Pb, Sn, Ag) at the crystal-vacuum interface. Charge neutrality would be maintained by having protons react with structural oxygen to form hydroxyl-like groups.

Similar reduction processes are likely to occur for Cu^{2+} in β''-alumina. The samples used in the experiments were equilibrated with ambient atmosphere enabling the crystals to hydrate. The decrease in EPR signal for Cu^{2+} is a clear indication that the annealing conditions are sufficient to cause reduction. There is no evidence that copper volatilized from the lattice as the crystals were crack-free and maintained the β''-alumina structure.

It is interesting to note that the copper β''-alumina crystals were transparent after heat treatment at 973 K while the crystals of Ag, Pb and Sn β''-alumina were deeply coloured. This disparity suggests that the final species present in the conduction plane are different for the two cases. In the present work, Cu^- is most likely the principal species as green luminescence has been observed in heat-treated materials. In contrast, metal clusters have been proposed for the other systems.[13]

3.2 EPR of Cu^{2+}(I)

The Cu^{2+}(I) species represent more than 90% of the total Cu^{2+} content in the material. Thus, the most significant EPR results concern this species rather than Cu^{2+}(II) or Cu^{2+}(III). The discussion that follows focuses on the site occupied by Cu^{2+}(I).

The EPR spectrum for Cu^{2+}(I) has been studied in unannealed samples in order to minimize contributions of the other sites. Cu^{2+}(II) and Cu^{2+}(III). The hyperfine structure of Cu^{2+}(I) is unresolved only when B_0 is parallel to the c axis. For an arbitrary orientation of B_0, the spectrum is

composed of several partially overlapping lines. In order to obtain the spin Hamiltonian parameters which are necessary to identify site I, angular variations were performed by rotating the crystal around two orthogonal crystallographic axes. An accurate determination of the magnetic parameters was made possible by comparing the experimental angular variations with calculated ones. Fig. 2 shows the results obtained for rotation in the (basal) *ab* plane. The principal features are as follows: (*a*) two *g*-tensor axes (labelled *z* and *y*) lie in the *ab* plane; the third axis (*x* axis) is thus collinear to the *c* axis, as confirmed by the angular variation in the *ca* plane (not shown); (*b*) there are three magnetically distinct sets of Cu^{2+}(I) sites, with *z* axes separated by 120°; (*c*) each *z* axis makes an angle of *ca.* 5° with respect to the *a* axis; this non-coincidence of magnetic and crystallographic axes is responsible for site splitting of the EPR spectrum. The spin Hamiltonian parameters of Cu^{2+}(I) are reported in Table 1. Owing to the lack of resolution for $B_0 \| c$, the value $A_x \leq 20 \times 10^{-4}$ cm^{-1} for the hyperfine coupling was deduced from a simulation of the experimental lineshape (Fig. 1) using the sum of four Gaussian lines having the same widths as those measured for the EPR lines in the *ab* plane.

No attempt was made to study the minor sites, Cu^{2+}(II) and Cu^{2+}(III). In addition to representing only a small fraction of the Cu^{2+} content, their angular variations were complicated by contributions of other signals: Cu^{2+}(I) and Cu^{2+}(III) in the case of Cu^{2+}(II), and Cu^{2+}(II) and Mn^{2+} impurities in the case of Cu^{2+}(III).

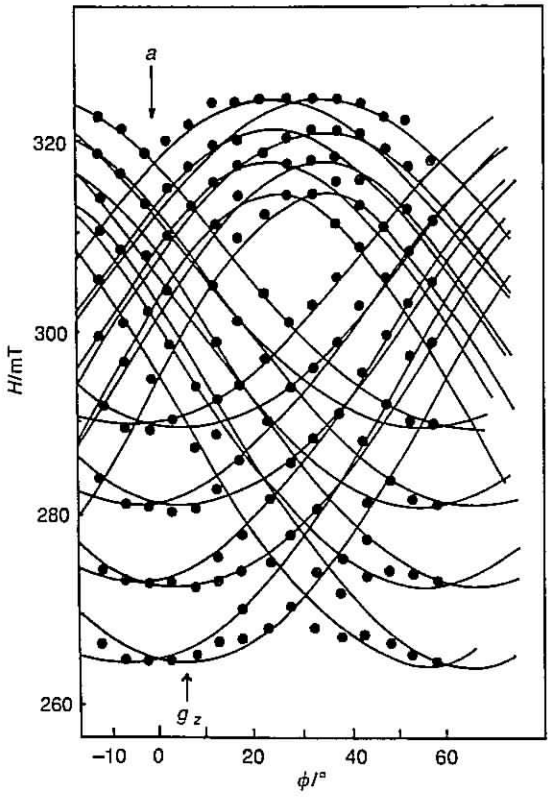

Fig. 2 Angular variation in the *ab* plane for the Cu^{2+}(I) EPR spectrum. $\phi = 0$ corresponds to $B_0 \| a$. Experimental points are represented by circles, and full lines represent the angular variation calculated with the following parameters: $g_z = 2.385$, $A_z = 91 \times 10^{-4}$ cm^{-1}, $g_y = 2.072$ and $A_y = 32 \times 10^{-4}$ cm^{-1}. The site splitting is due to a deviation of the g_z axis from the *a* axis by *ca.* 5°

Table 1 Spin Hamiltonian parameters of Cu^{2+}(I)

g_x	g_y	g_z	A_x/cm^{-1}	A_y/cm^{-1}	A_z/cm^{-1}
2.097	2.072	2.385	$\leq 20 \times 10^{-4}$	32×10^{-4}	91×10^{-4}

3.3 Identification of the Cu^{2+}(I) site

The two types of site available in the conduction plane of β''-alumina are the four-co-ordinated Beevers–Ross (BR) site and the eight-co-ordinated mO site. The BR site is an axially compressed tetrahedral site with C_{3v} symmetry, the C_3 axis parallel to the *c* axis. Based on the measured lattice parameter of Cu^{+}/Cu^{2+} β''-alumina, it is possible to calculate the various bond lengths in the structure.[14] The fact that c_0 for the copper samples (33.48 Å) is similar to that of Na^{+} β''-alumina suggests that the distance will be comparable in the two isomorphs. The short BR—O(3) bond length (along the C_3 axis) is *ca.* 2.26 Å, while the three other BR—O(4) bond lengths are *ca.* 2.75 Å. In regular T_d symmetry, the d orbitals of Cu^{2+} split into a low-lying doublet, e, and a higher energy triplet, t_2. A lowering of the symmetry to C_{3v} splits the t_2 set into a singlet $a_1(d_{z^2})$ and a doublet $e(d_{xz},d_{yz})$, the *z* axis being parallel to the c axis. Since the compression occurs along the C_3 axis, the d_{z^2} orbital is the most destabilized and the energies of the d orbitals are in the order $a_1(d_{z^2}) > e(d_{xz},d_{yz}) > e(d_{xy},d_{x^2-y^2})$. As a consequence, the electron ground state of Cu^{2+} in a BR site is $^2A_1$. The *g* tensor should reflect the nature of this ground state and the *g* values should be expressed as[15]

$$g_{\parallel} = g_z = g_e$$
$$g_{\perp} = g_x = g_y = g_e - 2\lambda/\delta \qquad (1)$$

where λ is the effective spin–orbit coupling constant and δ is the energy separation between $a_1(d_{z^2})$ and $e(d_{xz,yz})$ levels. This expression implies $g_{\perp} > g_{\parallel} \approx 2.00$ with the g_z axis along the *c* axis. The experimentally observed sequence is $g_z > g_x, g_y > 2.00$ with the g_z axis aligned perpendicular to the *c* axis. The experimental results are, therefore substantially different from what is expected for a BR site.

The second possible site is the eight-co-ordinated mO site with C_{2h} symmetry (Fig. 3). The various mO–oxygen distances will be:[14] mO—O(5) ≈ 2.81 Å (multiplicity 2), mO—O(3) ≈ 2.78 Å (multiplicity 2) and mO—O(4) ≈ 2.76 Å (multiplicity 4). In order to predict qualitatively the sequence of *g* factors and the g_z orientation, the co-ordination polyhedron at the mO site is considered as a superposition of two distorted square-planar polydehra. One polyhedron forms a lozenge composed of two O(5) and two O(3) atoms. The second configuration is rectangular and is formed by the four O(4) atoms (Fig. 3). In the following discussion of each polyhedron, the in-plane axes are defined as the *x* and *y* axes. Among the five d orbitals, only those lying in the *xy* planes will be strongly affected by the crystal field.

For the lozenge, the angle between the O(5)—O(5) and O(3)—O(3) directions is 90°. Thus, the lobes of the $d_{x^2-y^2}$ orbital for Cu^{2+} point toward O(5) and O(3) atoms while the lobes of the d_{xy} orbital point between these atoms. The result is a strong destabilization of the $d_{x^2-y^2}$ orbital. For the rectangular geometry, the lobes of the $d_{x^2-y^2}$ orbital point between the mO—O(4) directions, so that it is not destabilized. Moreover, the O(4)—mO—O(4) angle is different from 90° so that the lobes of the d_{xy} orbital deviate from the mO—O(4) directions and its destabilization will be weaker than in the lozenge case. If the two co-ordination polyhedra are superimposed, the most destabilized orbital should be the $d_{x^2-y^2}$ contained in the plane formed by O(5) and O(3) atoms. The unpaired electron is thus localized in this orbital, and approxi-

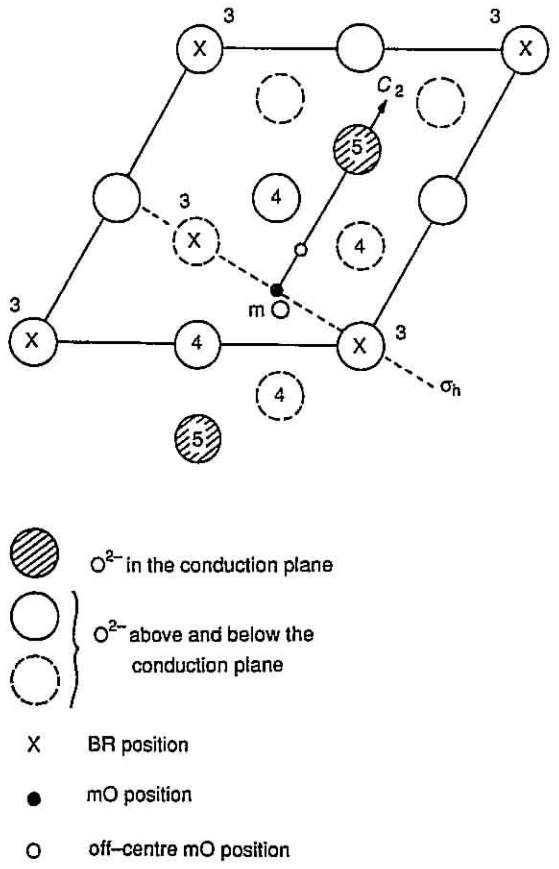

Fig. 3 Schematic representation of the conduction plane and the oxygen layers above and below showing the off-centre mO position. The splitting of the O(5) position (not represented on the figure) may be responsible for the site splitting of the EPR spectrum

mate expressions for the g factors are given by:[15]

$$g_z \approx g_e - 8\lambda/\Delta_{xy}$$
$$g_x \approx g_e - 2\lambda/\Delta_{yz}$$
$$g_y \approx g_e - 2\lambda/\Delta_{xz} \quad (2)$$

where Δ_{xy}, Δ_{yz} and Δ_{xz} are the energy separations between the $d_{x^2-y^2}$ orbital and the d_{xy}, d_{yz} and d_{xz} orbitals. In this case the expected sequence is $g_z > g_x g_y > 2.00$ with the z axis orthogonal to the plane containing O(5) and O(3) atoms. That is, g_z points between the c axis and the ab plane. It is important to note that this representation is exactly what was experimentally determined for Na^+/Cu^{2+} β''-alumina.[11] However, it is not consistent with the observed results for Cu^+/Cu^{2+} β''-alumina. Although the experimental sequence of g factors in the present study is the same as the theoretical one, the observed g_z axis orientation, along the O(5)—O(5) direction, is in disagreement with the expected one between the c axis and the ab plane. Thus, while it appears that Cu^{2+} occupies the equilibrium mO position in Na^+/Cu^{2+} β''-alumina, the EPR results indicate that the Cu^{2+} is slightly displaced from this site in Cu^+/Cu^{2+} β''-alumina.

An off-centre mO position, with displacement along the mO—O(5) direction is shown in Fig. 3. This position reduces the site symmetry to C_2 and the g_z axis will now be along the direction of displacement. The co-ordination is reduced to five in this off-centre position since one Cu^{2+}—O(5) and two Cu^{2+}—O(4) bonds are shortened. The co-ordination polyhedron of Cu^{2+}(I) is now similar to a distorted square pyramid with C_2 symmetry. This configuration should produce d orbital energies in the sequence $d_{x^2-y^2} > d_{z^2} > d_{xy} > d_{xz}, d_{yz}$.[16] The g values for the off-centre mO site will not vary appreciably from those given in eqn. (2) which leads to $g_z > g_x g_y > 2.00$ with the z axis parallel to the mO—O(5) direction (*i.e.* the crystallographic *a* direction). The expected behaviour of an off-centre position agrees well with the EPR results. In addition, it is interesting to note that the site splitting of the g_z axis (Fig. 2) is probably associated with the splitting of the O(5) distribution commonly observed in these compounds.[2,5]

The EPR results for Cu^{2+} in a distorted square-pyramidal site (C_{2h} symmetry) in $(NH_4)_2SO_4$ indicate very similar behaviour to that of the Cu^{2+}(I) in β''-alumina.[17] In the present work the ratio $R = g_z A_z$ was found to be $R = 261$ cm for Cu^{2+}(I). The corresponding value in ammonium sulphate is $R = 245$ cm. By comparison, R is very high (960 cm) in an undistorted tetrahedron and relatively small in both distorted octahedra ($R < 200$ cm) and square-planar configuration ($R \approx 100$ cm). Although the R value is very close to that found in a distorted square-pyramidal geometry, it should also be noted that R values in the range 200–250 cm have been obtained in various pseudotetrahedral complexes.[18] This is also consistent with the present model where it can be seen from Fig. 3 that the co-ordination polyhedron formed by two O(3) and two O(4) atoms resembles a flattened tetrahedron.

3.4 Comparison with Na^+/Cu^{2+} β″-Alumina

The preceding section indicated that the results obtained for Na^+/Cu^{2+} β''-alumina were different from those described in the present work for Cu^+/Cu^{2+} β''-alumina. The principal differences concern two points: the site occupied by Cu^{2+} and the temperature dependence of the EPR spectra.

In unannealed Na^+ Cu^{2+} β''-alumina, Cu^{2+} occupies a site ascribed to the mO site. It is characterized by the following parameters: $g_\parallel \approx 2.310$, $g_\perp \approx 2.053$, $A_\parallel \approx 156 \times 10^{-4}$ cm^{-1} and $A_\perp \approx 16 \times 10^{-4}$ cm^{-1}, with the z axis perpendicular to the plane containing O(3) and O(5) atoms, as expected for the equilibrium mO site. Annealing treatments result in the development of a new EPR spectrum with 'reversed' g factors (*i.e.* $g_\parallel < g_\perp$): $g_\parallel \approx 2.003$, $g_\perp \approx 2.240$, $A_\parallel \approx 93 \times 10^{-4}$ cm^{-1} and $A_\perp \approx 92 \times 10^{-4}$ cm^{-1}. This spectrum has been ascribed to an mO site perturbed by Na^+ vacancies.[11] The present work suggests that the localization of Cu^{2+} is influenced by the nature of the mobile ions, Na^+ or Cu^+, in the conduction plane. The shift of the Cu^{2+} position from the equilibrium mO site may be related to the fact that Na^+ occupies essentially BR sites,[1,2] while Cu^+ occupies both BR and mO sites.[9] Regardless of the precise mechanism, it is evident that Cu^{2+} shows strong preference for mO sites (theoretical or off-centre) independent of the copper content in β''-alumina.

The EPR spectra of Na^+/Cu^{2+} β''-alumina are intense and well resolved only at liquid helium temperature while they are almost unaffected by temperatures between 4 and 300 K in Cu^+/Cu^{2+} β''-alumina. This difference may be associated with the mobile (monovalent) ions in the conduction plane. Ionic conductivity for Na^+ β''-alumina is substantially greater ($\sigma_{RT} \approx 1 \times 10^{-2}\ \Omega^{-1}$ cm^{-1}) than the value measured for Cu^+ Cu^{2+} β''-alumina at room temperature ($\sigma_{RT} \approx 2 \times 10^{-8}\ \Omega^{-1}$ cm^{-1}).[19] The rapid motion of Na^+ in the neighbourhood of Cu^{2+} could produce two temperature-dependent effects. First, it may modulate the crystal field of Cu^{2+}, which should in turn, shorten the spin–lattice relaxation time. With increasing temperature the EPR lines would then broaden significantly. The second possibility is that rapid Na^+ motion could induce local Cu^{2+} hopping from site to site, in the conduction plane. This type of local transport was proposed previously to explain the random type spectrum

observed in Na^+/Cu^{2+} β''-alumina.[11] These temperature-dependent effects do not appear in Cu^+/Cu^{2+} β''-alumina because of the greatly reduced motion of Cu^+ ions.

4. Conclusions

Samples of Cu^+/Cu^{2+} β''-alumina containing *ca.* $2–5 \times 10^{20}$ Cu^{2+} per cm^3 were studied by EPR. Heat treatments at temperatures above 773 K greatly decreased the Cu^{2+} content and above 1073 K complete reduction was observed. The combination of EPR and optical spectroscopy suggests that Cu^+ was produced from the annealing treatments. It is likely that the presence of water in the conduction plane of the crystal played an important role in the reduction reaction.

The EPR spectra were also used to identify the site occupied by Cu^{2+}. More than 90% of the Cu^{2+} ions occupy an off-centre mO position arising from the displacement of Cu^{2+} along the mO—O(5) direction. A small quantity of Cu^{2+} ions were found to occupy two other sites which were not identified. Spectral differences between Cu^+/Cu^{2+} β''-alumina and Cu^{2+}/Na^+ β''-alumina suggest that the nature and mobility of the monovalent ion in the conduction plane influence the EPR response.

The research was supported by the U.S. Office of Naval Research, the Franco-American Commission for Cultural Exchange and NATO (collaborative grant 890337). The authors thank T. Faltens and D. Simons for technical assistance.

References

1 B. Dunn, G. C. Farrington and J. O. Thomas, *MRS Bull.*, 1989, **14**, 22.
2 G. C. Farrington, B. Dunn and J. O. Thomas, *High Conductivity Solid Ionic Conductors*. ed. T. Takahashi, World Scientific, Singapore, 1989, p. 327.
3 A. J. Alfrey, O. M. Stafsudd, D. L. Yang, B. Dunn and L. Salmon, *J. Chem. Phys.*, 1988, **88**, 707.
4 M. A. Saltzberg and G. C. Farrington, *J. Solid State Chem.*, 1989, **83**, 272.
5 W. Carillo-Cabrera, J. O. Thomas and G. C. Farrington, *Solid State Ionics*, 1988, **28–30**, 317.
6 B. Dunn, D. L. Yang and D. Vivien, *J. Solid State Chem.*, 1988, **73**, 235.
7 J. D. Barrie, L. A. Momoda, B. Dunn, D. Gourier, G. Aka and D. Vivien, *J. Solid State Chem.*, 1990, **86**, 94.
8 J. D. Barrie, B. Dunn, O. M. Stafsudd and P. Nelson, *J. Lumin.*, 1987, **37**, 303.
9 J. D. Barrie, B. Dunn, G. Hollingsworth and J. I. Zink, *J. Phys. Chem.*, 1989, **93**, 3958.
10 G. Hollingsworth, J. D. Barrie, B. Dunn and J. I. Zink, *J. Am. Chem. Soc.*, 1988, **110**. 6569.
11 L. Abello, S. J. Schwerdtfeger and C. F. Schwerdtfeger, *Phys. Status Solidi B*, 1984, **125**, 333.
12 J. A. Little and D. J. Fray, *Fast Ion Transport in Solids* ed. P. Vashista, J. Mundy and G. Shenoy, North-Holland, Amsterdam 1979, p. 323.
13 G. S. Rohrer and G. C. Farrington, *Chem. Mater.*, 1989, **1**, 438.
14 J. O. Thomas, personal communication.
15 J. E. Wertz and J. R. Bolton, *Electron Spin Resonance*, McGraw Hill, New York, 1972.
16 J. K. Burdett, *Adv. Inorg. Chem. Radiochem.*, 1978, **21**, 113.
17 S. K. Hoffman, *Acta Phys. Pol. A*, 1976, **46**, 253.
18 H. Yokoi and A. W. Addison, *Inorg. Chem.*, 1977, **16**, 1341.
19 L. G. Salmon, M. S. Thesis, University of California, Los Angeles, 1986.

Paper 0/04793G; *Received 24th October*, 1990